Digital Gabor Filters Do Generate MRA-based Wavelet Tight Frames

Hui Ji[a,*], Zuowei Shen[a], Yufei Zhao[a]

[a]*Department of Mathematics, National University of Singapore, Singapore 117543*

Abstract

Gabor frames, especially digital Gabor filters, have long been known as indispensable tools for local time-frequency analysis of discrete signals. With strong orientation selectivity, tensor products discrete (tight) Gabor frames also see their applications in image analysis and restoration. However, the lack of multi-scale structures existing in MRA-based wavelet (tight) frames makes discrete Gabor frames less effective on modeling local structures of signals with varying sizes. Indeed, historically speaking, it was the motivation of studying wavelet systems. By applying the unitary extension principle on some most often seen digital Gabor filters (e.g. local discrete Fourier transform and discrete Cosine transform), we are surprised to find out that these digital filter banks generate MRA-based wavelet tight frames in square integrable function space, and the corresponding refinable functions and wavelets can be explicitly given. In other words, the discrete tight frames associated with these digital Gabor filters can be used as the filter banks of MRA wavelet tight frames, which introduce both multi-scale structures and fast cascade implementation of discrete signal decomposition/reconstruction. Discrete tight frames generated by such filters with both wavelet and Gabor structures can see their potential applications in image processing and recovery.

Keywords: tight frame, multiresolution analysis, Gabor frame

1. Introduction

Gabor frames and wavelet frames are two types of most commonly used systems in signal and image processing, restoration and analysis. For years, Gabor system has been a pervasive tool for local time-frequency analysis of signals, with a wide range of applications in signal processing, texture analysis, image processing and many others. There are two main advantages of Gabor systems over other systems in signal/image processing. One is the optimality in the sense of minimizing the joint uncertainty in the combined time-frequency space, and the other is the strong orientation sensitivity that gives a strong response for locations of images that have structures in the given direction. When being applied to process digital discrete signals, Gabor systems usually are employed either in the form of filters or in the form of blocked systems. In image processing, Gabor filters are used as linear filters for edge detection, texture representation and discrimination. The blocked systems are constructed by dividing the signals into different blocks (windows) and then decomposing signals of each block over some local basis ([1, 2]). The most often seen local basis is *discrete Fourier transform* (DFT) or *discrete Cosine transform* (DCT) which is real-valued version of DFT with double length and half-sample phase shift. Recently, a class of discrete Gabor frames are proposed in [3] for image recovery, owing to their strong orientation selectivity. However, all these discrete Gabor bases/frames lack a very important structure existing in wavelet bases/frames: the multi-scale structure of affine systems that provides a multi-resolution analysis (MRA) in associated square integrable function space. The multi-scale structure is very effective on modeling local structures with different sizes often seen in 2D images, and the MRA is for straightforward derivations and connections between digital tight frames for discrete signals and wavelet tight frames for square integrable functions, together with fast cascade implementation of decomposition and reconstruction. In

*Corresponding author

Email addresses: matjh@nus.edu.sg (Hui Ji), matzuows@nus.edu.sg (Zuowei Shen), a0086274@nus.edu.sg (Yufei Zhao)

recent years, wavelet tight frames have seen their wide applications in image recovery; see e.g. [4, 5, 6, 7]. In most existing applications, both digital Gabor frames and wavelet frames are implemented via a filter bank approach, either Gabor digital filter bank or wavelet filter bank. In this paper, we show that the most often seen Gabor digital filter banks or local Cosine digital filter banks in many applications do generate wavelet digital filter banks, i.e. filter banks of refinement masks and wavelet masks, that lead to multiresolution analysis based (MRA-based) wavelet tight frames in square integrable spaces. This automatically builds the multiresolution analysis into Gabor and local Cosine systems. This result is part of our efforts to bridge the gap between Gabor systems and wavelet frames.

1.1. Discussions and Motivations

The desire of understanding the deep connections between Gabor frames and wavelet frames came from extensive works done in wavelet tight frame and Gabor frame based image restoration methods. The multi-scale structure and efficient filter bank-based numerical implementation make digital wavelet tight frame very appealing to image recovery, particularly with the prevalence of ℓ_1-norm relating regularizations for inverse problems. For example, shift-invariant Daubechies' wavelets [4] and dual-tree complex wavelets [8] have been used in image analysis and denoising. Spline wavelet tight frames [9] have been used as the preferred sparsifying systems of images for solving many recovery problems, including non-blind and blind image in-painting [5, 10], non-blind and blind image deblurring [6, 11]. Also, spline wavelet tight frames also have been used for volume data recovery in medical imaging and cryo-EM imaging [12, 13]. Recently, data-driven wavelet tight frames and non-local wavelet frames are developed and used in various image recovery tasks [14, 15]. Indeed, it is shown in [16] that the wavelet frame based ℓ_1-norm relating regularization can be seen as sophisticated discretization of minimizations involving the total variation penalty. Interesting readers are referred to [17, 18, 19]. Recently, a class of discrete Gabor frames are proposed in [3] for image recovery, owing to their strong orientation selectivity. The algorithm developed in [3] outperforms those methods which also adopt directional wavelets (e.g. dual-tree complex wavelets [8]). However, it is known that the multi-resolution structure of wavelet systems allows one to decompose images in multi-scale levels, which is very helpful to model image features with varying sizes. This makes us to wonder whether Gabor filter banks have some hidden structures that were not carefully studied. It might be that some of Gabor filter banks implicitly carry a multiresolution structure. This is the first motivation that inspires our adventure in this paper.

In fact, the studies on digital discrete frames/tight frames with emphasis on connections of both wavelet and Gabor structures have been scant in the literature. A continuous Gabor wavelet transform for $L_2(\mathbb{R}^2)$ is introduced in [20], which extends continuous wavelet transform by using the set of Gabor functions as mother wavelets. The system for $L_2(\mathbb{R}^2)$ is defined by the discretization of the transform in the phase space. Numerical simulation done in [20] indicates that the systems obtained via such a discretization form frames for $L_2(\mathbb{R}^2)$, provided that the sampling in the phase space is sufficiently dense. In the context of image in-painting, a set of discrete tight frames is developed in [21] for vector space $\mathbb{R}^n$, in which, by the main result of this paper, the first column of a local DCT with dimensionality p can be viewed as the refinement mask of the MRA for p-dilation Haar wavelets and the other columns can be viewed as wavelet masks. Then, by the orthogonality of local DCT, a wavelet tight frames can be obtained for $\mathbb{R}^n$ via the standard discretization of p-dilation Haar wavelet frames.

It is well known that wavelet systems associated with Gabor functions are closely related to signal processing mechanism in human visual perception. It is shown in Daugmann [22] that simple cells in the visual cortex of mammalian brains can be modeled by a wavelet system,

$$\{\psi_\ell(2^j \cdot -k)\}_{0\le \ell\le L, j\in\mathbb{Z}, k\in\mathbb{Z}^2},$$

where $\{\psi_\ell\}$ is a set of 2D Gabor functions with varying frequency orientations. To be used in real applications, the digitalization of such wavelet systems is done by directly sampling the atom functions of the system on a discrete grid (e.g. [20]) in time-frequency plane. The digital discrete wavelet systems obtained via such a sampling approach cannot guarantee many important properties needed in signal processing, e.g., tight frame property and fast cascade implementation of signal decomposition/reconstruction. This shows another need of establishing a connection between digital Gabor and wavelet frame filters.

Indeed, in function space, the lack of multi-scale structure of continuous Gabor transform and Gabor systems was the motivation of studying continuous wavelet transform and wavelet systems; see e.g.

[23, 24]. The origin of Gabor systems comes from the so-called windowed Fourier transform first proposed by Gabor [25] for measuring local frequency variations of signals:

$$\mathcal{S}f(u,\xi) = \int_{\mathbb{R}} f(x)\overline{g_{u,\xi}(x)}dx = \int_{\mathbb{R}} f(x)\overline{g(x-u)e^{i\xi x}}dx, \quad f \in L_2(\mathbb{R}),$$

where g is a symmetric real-valued window function, e.g., Gaussians. It can be seen that the window sizes of all atoms $g_{u,\xi}$ are the same, and thus they can not be used for analyzing structures of signals with different sizes. By using time-frequency atoms with varying support sizes, the continuous wavelet transform defined from the translations and dilations of some mother wavelet ψ with $\widehat{\psi}(0) = 0$:

$$\mathcal{W}f(u,s) = s^{-1/2}\int_{\mathbb{R}} f(x)\overline{\psi_{u,s}(x)}dx = s^{-1/2}\int_{\mathbb{R}} f(x)\overline{\psi(s^{-1}(x-u))}dx, \quad f \in L_2(\mathbb{R}),$$

is then proposed for analyzing signals. Both Gabor transform and wavelet transform have simple reconstruction/inverse transform with very mild conditions on the window or mother wavelet. The well-known *Morlet wavelet transform* [23] used a modified version of Gabor function as the mother wavelet

$$\psi_\xi(x) = c_\xi e^{-\frac{1}{2}x^2}(e^{i\xi x} - e^{-\frac{1}{2}\xi^2}).$$

It can be seen that Morlet wavelet indeed provides some connections between these two transforms.

As only sample data of these two operators is available in practice, it leads to consider Gabor systems and wavelet systems. A Gabor system is generated via discretizing shifts of the window function in time-frequency plane:

$$X = (K,L)_g = \{g(x-u)e^{i2\pi\eta x}\}_{u\in K,\eta\in L},$$

where both K and L are the sequences in $\mathbb{R}$. Particularly, when $K \times L \subset \mathbb{R}\times\mathbb{R}$ is a lattice, a *Gabor system* $X = (K,L)_g \in L_2(\mathbb{R})$ is composed of translations and modulations of g on lattices $K \times L$, i.e. $X = (K,L)_g = \{g(x-k)e^{-2\pi i\ell x}\}_{k\in K,\ell\in L}$. Consider a uniform time-frequency lattice set $K\times L = a\mathbb{Z}\times b\mathbb{Z}$ $(a,b \in \mathbb{R}^+)$. Then, the Gabor system can be expressed as

$$X = (K,L)_g = \{g(x-ak)e^{-2\pi ib\ell x}, x \in \mathbb{R}\}_{k,\ell\in\mathbb{Z}}. \tag{1}$$

A wavelet system is generated via discretizing the dilation and translation, particularly for a given set of wavelet functions $\Psi = \{\psi_1, ..., \psi_r\} \subset L_2(\mathbb{R})$, the *p-dilation wavelet system* $X(\Psi)$ is composed of dilations and translations of these wavelet functions:

$$X(\Psi) = \{\psi_{\ell,n,k}\}_{\substack{1\le\ell\le r\\ n,k\in\mathbb{Z}}} = \{p^{n/2}\psi_\ell(p^n\cdot - k)\}_{\substack{1\le\ell\le r\\ n,k\in\mathbb{Z}}}. \tag{2}$$

Here, $p \in \mathbb{Z}^+$ with $p > 1$ is the *dilation factor* of $X(\Psi)$. If $p = 2$, $X(\Psi)$ is the so-called *dyadic wavelet system.*

One key question on defining a meaningful system is under what circumstances, this system, composed of the samples of either Gabor or wavelet transform, can be used to fully reconstruct the original function. The reconstruction capability of a system usually is much more complicated than that of its corresponding integral operator-based transform, since it requires the frame property. There has been an abundant literature on the studies of the frame/tight frame properties of Gabor systems and wavelet systems in square integrable function space; and how to construct good window functions, or wavelets that are appealing to applications. A complete survey of the literature goes beyond the scope of this paper. Instead, we only mention a few those are most related or those motivate our work. Among many discoveries, two very important principles are the duality principle for Gabor systems ([26, 27, 28, 29]) and the unitary extension principle for wavelet systems ([30]). These two principles not only give a characterization of Gabor frames and MRA-based wavelet frames, they also provide basic principles of constructing Gabor frames and MRA-based wavelet frames. For the construction of Gabor window functions, the famous painless construction [31] is the most important one, and many other constructions of Gabor window functions are related to the ideas given in [31], that is later linked to the duality principle. For the construction of wavelet systems, we only mention a few, i.e., band-limited orthonormal wavelet bases by Meyer [32], compactly supported orthonormal wavelet bases by Daubechies [33], biorthogonal

wavelet bases [34], and compactly supported spline tight wavelet frames [30]. The painless construction presented in [31] can be viewed as an elegant application of the duality principle (see e.g. [27, 35]), although the duality principle was discovered after the painless construction of Gabor window functions. The construction of wavelet systems took off after the discovery of multi-resolution analysis by Mallat and Meyer [36, 32]. Band-limited orthonormal wavelet bases [32], compactly supported orthonormal wavelet bases [33], biorthogonal wavelet bases [34] are all MRA-based non-redundant systems. The MRA-based redundant systems, tight frames and bi-frames, took off after the discovery of the unitary extension principle [30]. Compactly supported spline tight wavelet frames constructed in [30] are the first set of examples of MRA-based tight frames generated by the unitary extension principle.

As the duality principle and the unitary extension principle lay down the foundation on characterization of frame properties of Gabor system and MRA-based wavelet system respectively; and two principles play key roles in the construction of Gabor frame and MRA wavelet frame respectively, our efforts started from building up the connections of two principles. Recently, a connection between the duality principle and the unitary extension principle is established in [37, 35], which essentially gave an understanding of the unitary extension principle from the duality principle. This understanding was rooted back to the original ideas of the duality principle [27]. More specifically, recall that a dual Gramian matrix analysis was introduced in [38] for shift invariant systems to represent the frame operator in Fourier domain and an adjoint system was introduced for any given Gabor system in [26, 27]. In fact, the dual Gramian matrix analysis and the relations to Grammian matrix of its adjoint system is the key to any kind of duality analysis of frame systems in Hilbert space. The key discovery in [26, 27] is that the dual Gramian matrix of a given system equals to the Gramian matrix of its adjoint system. A similar discussion can be carried out for the mixed dual Gramian and Gramian matrices for a given system and its adjoint system and their dual systems. This is the duality principle of [26, 27]. As consequences, frame, tight frame and bi-frame properties of a system can be characterized by Riesz, orthogonality, and biorthogonality properties of its adjoint system. This, in turn, leads to the constructions of Gabor frames.

In the literature, this consequential result is often called the duality principle instead. The proofs in both [28, 29] are independent of and different from [27]. Both proofs in [28, 29] were based on Wexler-Raz identity and Wexler-Raz biorthogonal relation [39]. Both the Wexler-Raz identity and Wexler-Raz biorthogonal relation can be viewed as a special case and can be deduced from the fact that the (mixed) dual Gramian matrix of a system and its dual equals to the (mixed) Gramian matrix of its adjoint system and its dual (see e.g. [35]). For example, the Wexler-Raz biorthogonal relation essentially says that the (mixed) dual Gramian matrix of a system and its dual equals to the (mixed) Gramian matrix of its adjoint system and its dual, whenever both matrices are the identity. Hence, this connects tight frame or bi-frame properties of systems to orthogonality and bi-orthogonality of their adjoint systems.

This core idea of the complete version of duality principle, the dual Gramian matrix of a system equals to the Gramian matrix of its adjoint system, was further developed to the most general setting in [37, 35], which leads to the establishment of the connection of these two principles. The unitary extension principle [30] says tight frame property of a wavelet system is equivalent to tight frame property of a system generated by the filter bank in digital space. The condition imposed on the filter bank in UEP is the orthogonality of the adjoint system of the original system generated by the filter bank. Hence tight frame property of this system is ensured by the duality principle (see [37, 35] for details). This reveals the fundamental connection between two principles. This new understanding of both principles not only leads to many interesting constructions of Gabor frames and MRA-based wavelet frames in [37, 35] but also leads us to believe that some of Gabor filters can generate MRA wavelet frames that, in turn, leads to what we are discussing in this paper.

For numerical computation, one needs to further discretizing both Gabor systems and wavelet systems to digital systems. The digital Gabor system for digital space $\ell_2(\mathbb{Z})$ is done by uniformly sampling the atoms of the Gabor system on a discrete grid in time. The digital versions in $\ell_2(\mathbb{Z})$ of the atoms, i.e. $\{g(k)e^{i2\pi\eta k}\}_{\eta\in L}$, are often called digital Gabor filters. We note that when g is a compactly supported window function, the digital Gabor filters are finitely supported. In such a digitalization, the result of [27] says that under a very mild condition on the window g, the frame and tight frame properties of Gabor systems will be carried forward by the system generated by its digital Gabor filters in $\ell_2(\mathbb{Z})$. However, the inverse is not true, i.e. frame or tight frame properties of digital Gabor filters in digital space $\ell_2(\mathbb{Z})$ do not indicate the frame properties in square integrable function space of the original Gabor

system. The discretization of MRA-based wavelet systems is done by simply taking the filters, i.e. the filter bank consisting of refinement mask and wavelet masks, as generators of a system in digital space. Different from Gabor systems, under unitary extension principle, tight frame property of such a digital wavelet system guarantees tight frame property of the underlying wavelet system. Here we note that the orthogonality of the digital system dose not guarantee the orthogonality property of the original wavelet system. This also indicates that MRA is built for tight frame wavelet systems in a natural manner.

1.2. Summary of Discoveries

Motivated by the gap between digital discrete Gabor systems and MRA-based wavelet systems, this paper aims at investigating what is the connection between digital Gabor filters and MRA-based wavelet tight frames for $L_2(\mathbb{R})$. A surprising discovery is that a class of digital Gabor filters often seen in signal/image processing, i.e., DFT/DCT, is closely related to MRA-based wavelet tight frames for continuum space. Such a connection can be summarized as the following: these often see digital Gabor filters define MRA-based wavelet tight frames for $L_2(\mathbb{R})$ with different dilation factors. More specifically, consider a digital discrete Gabor system,

$$\{g(m-ak)e^{-2\pi ib\ell m}, m\in\mathbb{Z}\}_{k\in\mathbb{Z},\ell\in\{0,\dots,\frac{1}{b}-1\}}, \tag{3}$$

where g is a finitely supported discrete window sequence and a, b with $a, \frac{1}{b}\in\mathbb{N}^+$ are shift parameters. For a DFT-based orthonormal block basis, the window sequence is a constant vector, $\frac{1}{\sqrt{M}}[1,1\dots,1,1]$, over its support, and $a=\frac{1}{b}=M>1$. Such an orthonormal block basis is generated by the translations of the following M filters with step size M:

$$\{\sqrt{M}g_\ell(m)=\frac{1}{\sqrt{M}}e^{-2\pi ib\ell m}\}_{0\le\ell\le M-1}. \tag{4}$$

Consider an integer factorization of M, denoted by $M=p\cdot q$ with $p>1$. Our calculation showed that these M filters satisfy the following condition: for any $\mu\in p^{-1}\mathbb{Z}/\mathbb{Z}$,

$$\sum_{\ell=0}^{M-1}\widehat{g}_\ell(\omega)\overline{\widehat{g}_\ell(\omega+2\pi\mu)}=\delta(\mu),\quad \text{for all } \omega\in\mathbb{R}. \tag{5}$$

where $\delta(\mu)=1$ if $\mu=0$ and 0 otherwise. The condition (5) indeed is exactly UEP [30, 9] for the construction of MRA-based wavelet tight frames with dilation factor p. In other words, when using the filter g_0 as the mask for defining scaling function of MRA and $\{g_\ell\}_{\ell=1}^{M-1}$ as the masks for defining $M-1$ wavelets with dilation p:

$$\phi(\cdot)=p\sum_{m\in\mathbb{Z}}g_0(m)\phi(p\cdot-m);\quad \psi_\ell(\cdot)=p\sum_{m\in\mathbb{Z}}g_\ell(m)\phi(p\cdot-m),\quad \ell=1,\dots,M-1,$$

the wavelet system $\{p^{n/2}\psi_\ell(p^n\cdot-k)\}_{\substack{1\le\ell\le M-1\\ n,k\in\mathbb{Z}}}$ forms an MRA-based wavelet tight frame for $L_2(\mathbb{R})$. Furthermore, different integer factorizations of M generate different wavelet systems:

1. When M is factorized as $M=M\cdot 1$, the resulting wavelet system forms an orthonormal wavelet basis for $L_2(\mathbb{R})$, i.e., Haar wavelet with dilation M. The scaling function is the indicator function on unit interval, the same as standard dyadic Haar wavelet.
2. When M is an even integer and is factorized as $M=2\cdot\frac{M}{2}$, the resulting system forms a dyadic tight wavelet frame for $L_2(\mathbb{R})$. When $\frac{M}{2}>1$, the scaling function is no longer an indicator function.
3. When $M=p^n$ with $n>1$ and is factorized as $M=p\cdot p^{n-1}$, the resulting system forms a tight wavelet frame for $L_2(\mathbb{R})$ with dilation factor p, and the scaling function is a spline $\in C^{n-2}$.

The same observation also holds true for the filters associated with DCT:

$$\{g_\ell(m)=\frac{1}{\lambda_\ell}\cos(\pi b\ell(m+\frac{1}{2}))\}_{0\le\ell\le M-1}, \tag{6}$$

with $b = \frac{1}{M}$, $\lambda_0 = M$ and $\lambda_\ell = \frac{M}{\sqrt{2}}$ for $\ell \neq 0$. The main difference from DFT is that the resulting wavelet tight frames are real-valued functions.

The aforementioned observation regarding the connection between digital filters from DCT/DFT and MRA-based wavelet tight frames leads us to have a more detailed examination on the connection between discrete Gabor filters and MRA-based wavelet tight frames. In this paper, we presented a sufficient condition on the discrete Gabor filter that defines an MRA-based wavelet tight frame for $L_2(\mathbb{R})$. As a result, the digital discrete tight frames will have the same multi-scale structures as digital discrete MRA-based wavelet tight frames for $\ell_2(\mathbb{Z})$. Moreover, we showed that only those digital discrete systems generated by the digital filters of the form (4) can form compactly supported wavelet tight frames with MRA structure for $\ell_2(\mathbb{Z})$. The 2D tensor products of such discrete tight frames have inherent properties of both digital Gabor systems and wavelet systems, including (1) local time-frequency analysis capability of digital Gabor systems; (2) multi-scale structures induced by the MRA, and (3) fast numerical implementation of cascade signal decomposition/reconstruction scheme. The experiments carried in this paper also showed that the proposed 2D tight wavelet frames have their advantages over existing MRA-based wavelet tight frames, when being used in ℓ_1-norm relating regularizations for image recovery.

The remaining of this paper is organized as follows. Section 2 gives an introduction to the preliminary knowledge needed for the discussion and a brief discussion on some related works. The main body of Section 3 is devoted to the results about the UEP-based relationship between digital Gabor filters and MRA-based wavelet tight frames. Also, as a by-product, the construction of (tight) Gabor frames for $L_2(\mathbb{R})$ via the (square root of) the refinable function of an MRA is presented in this section. In Section 4, we apply the constructed tight wavelet frames in two image recovery tasks: image denoising and deconvolution.

2. Notations and Preliminaries

In this paper, we use $\mathbb{Z}, \mathbb{Z}^+, \mathbb{R}$ to denote the set of integers, positive integers and real numbers, respectively. For any function $f \in L_2(\mathbb{R})$, its Fourier transform is defined by

$$\widehat{f}(\xi) = \int_{\mathbb{R}} f(x) e^{-i\xi x} dx, \quad \xi \in \mathbb{R}.$$

For any sequence $h \in \ell_2(\mathbb{Z})$, its Fourier series is defined by

$$\widehat{h}(\xi) = \sum_{k \in \mathbb{Z}} h(k) e^{-ik\xi}, \quad \xi \in \mathbb{R}.$$

We first introduce some concepts and notations related to frames and tight frames. Suppose H is a Hilbert space, e.g., $L_2(\mathbb{R})$ or $\ell_2(\mathbb{Z})$, with usual inner product $\langle \cdot \rangle$ and 2-norm $\| \cdot \|$. A system $\{v_n\}_{n \in I} \subset H$ is called a *frame* for H if there exist constants $0 < A \leq B < +\infty$ such that for any $f \in H$,

$$A\|f\|^2 \leq \sum_{n \in I} |\langle f, v_n \rangle|^2 \leq B\|f\|_2^2.$$

If $A = B = 1$, the frame $\{v_n\}_{n \in I}$ becomes a *tight frame*. For a frame $\{v_n\}_{n \in I}$, there exists a *dual frame* $\{u_n\}_{n \in I}$, such that any element f in H can be expressed as

$$f = \sum_{n \in I} \langle f, v_n \rangle u_n = \sum_{n \in I} \langle f, u_n \rangle v_n.$$

If $\{v_n\}_{n \in I}$ is a frame for H, the frame operator S defined as

$$S : H \to H, \ Sf = \sum_{n \in I} \langle f, v_n \rangle v_n$$

is well-defined in the sense of being bounded and invertible. The system $\{S^{-1} v_n\}_{n \in I}$ is a dual frame of $\{v_n\}_{n \in I}$, which is called the canonical dual frame. The canonical dual frame of a tight frame is itself.

Given a fixed window function $g \in L_2(\mathbb{R})$ and lattices $K \times L \subset \mathbb{R} \times \mathbb{R}$, a *Gabor system* $X = (K, L)_g \in L_2(\mathbb{R})$ is composed of translations and modulations of g on lattices $K \times L$, i.e. $X = (K, L)_g = \{g(x-k)e^{-2\pi i\ell x}\}_{k\in K,\ell\in L}$. Consider a uniform time-frequency lattice set $K \times L = a\mathbb{Z} \times b\mathbb{Z}$ $(a, b \in \mathbb{R}^+)$. Then, the Gabor system can be expressed as

$$X = (K, L)_g = \{g(x-ak)e^{-2\pi ib\ell x}, x \in \mathbb{R}\}_{k,\ell\in\mathbb{Z}}. \tag{7}$$

Interesting readers are referred to [40, 27, 41] for more details on the characterizations of frame and tight frame properties of the system (7). Digital discrete Gabor frames for $\ell_2(\mathbb{Z})$ are usually obtained by directly sampling continuous Gabor frames for $L_2(\mathbb{R})$ using shift parameters a, b with $a, \frac{1}{b} \in \mathbb{N}^+$:

$$\{g(m-ak)e^{-2\pi ib\ell m}, m \in \mathbb{Z}\}_{k\in\mathbb{Z},\ell\in\{0,\ldots,\frac{1}{b}-1\}}. \tag{8}$$

Many different conditions have been proposed for guaranteeing the (tight) frame properties of digital discrete Gabor systems of the form (8). Interesting readers are referred to [39, 42, 43, 3] for more details.

The construction of wavelet tight frames often starts with the construction of MRA, which is built on refinable function. A function $\phi \in L_2(\mathbb{R})$ is called *p-refinable* for $p \in \mathbb{Z}^+$ with $p > 1$, if

$$\phi(x) = p\sum_{k\in\mathbb{Z}} a_0(k)\phi(px-k), \quad x \in \mathbb{R}, \tag{9}$$

for some $a_0 \in \ell_2(\mathbb{Z})$, or equivalently $\widehat{\phi}(p\xi) = \widehat{a_0}(\xi)\widehat{\phi}(\xi), \xi \in \mathbb{R}$. The sequence a_0 is called the *refinement mask* of ϕ. Given a refinable function $\phi \in L_2(\mathbb{R})$ with $\widehat{\phi}(0) \neq 0$, the sequence of sub-spaces $\{V_n\}_{n\in\mathbb{Z}}$ defined by

$$V_n = \overline{span\{\phi(p^n \cdot -k)\}}_{k\in\mathbb{Z}}. \tag{10}$$

forms an MRA for $L_2(\mathbb{R})$ if it satisfies

$$\text{(i) } V_n \subset V_{n+1},\ n \in \mathbb{Z}, \quad \text{(ii) } \overline{\cup_n V_n} = L_2(\mathbb{R}), \quad \text{(iii) } \cap_n V_n = \{0\}.$$

Given an MRA generated by the refinable function ϕ, we can define a set of framelets $\Psi = \{\psi_\ell\}_{\ell=1}^r$ by

$$\psi_\ell(x) = p\sum_{k\in\mathbb{Z}} a_\ell(k)\phi(px-k), \quad x \in \mathbb{R}, \tag{11}$$

or equivalently $\widehat{\psi_\ell}(p\xi) = \widehat{a_\ell}(\xi)\widehat{\phi}(\xi), \xi \in \mathbb{R}$, for some sequences $\{a_\ell\}_{\ell=1}^r \subset \ell_2(\mathbb{Z})$. The sequences $\{a_\ell\}_{\ell=1}^r$ are called *wavelet masks* of the framelets $\{\psi_\ell\}_{\ell=1}^r$.

The UEP ([30, 9]) provides a sufficient condition on refinement mask a_0 and wavelet mask $\{a_\ell\}_{\ell=1}^r$ such that the p-dilation wavelet system $X(\Psi)$ defined by

$$X(\Psi) = \{p^{n/2}\psi_\ell(p^n \cdot -k)\}_{1\le\ell\le r,n,k\in\mathbb{Z}} \tag{12}$$

forms a tight frame for $L_2(\mathbb{R})$. For simplicity, this paper only consider the case where the refinement mask a_0 is finitely supported.

Theorem 1 (UEP [30])**.** *Let ϕ be a refinable function with $\widehat{\phi}(0) \neq 0$ and with finitely supported mask a_0. For a given $\Psi = \{\psi_\ell,\ \ell = 1, \ldots, r\}$ defined by* (11) *with wavelet masks $\{a_\ell\}_{\ell=1}^r$, the wavelet system $X(\Psi)$ defined by* (12) *forms a tight frame of $L_2(\mathbb{R})$, if the masks $\{a_0, a_1, \ldots, a_r\}$ satisfy*

$$\sum_{\ell=0}^{r} \widehat{a_\ell}(\xi)\overline{\widehat{a_\ell}(\xi + 2\pi\mu)} = \delta(\mu), \quad a.e.\ \xi \in \mathbb{R}, \tag{13}$$

for any $\mu \in p^{-1}\mathbb{Z}/\mathbb{Z}$.

Condition (13) can also be expressed as quadratic constraints:

$$\sum_{\ell=0}^{r}\sum_{n\in\Omega_j} \overline{a_\ell(n)}a_\ell(n+m) = p^{-1}\delta_{m,0} \tag{14}$$

for all $m \in \mathbb{Z}$, $j \in \mathbb{Z}/p\mathbb{Z}$, where $\Omega_j = (p\mathbb{Z}+j) \cap \mathrm{supp}(a_0)$. Here we mention that (14) is exactly the orthogonality of the adjoint system of a frame system generated by filter banks that must be a tight frame in sequence space to make sure that the corresponding wavelet system is a tight frame in $L_2(\mathbb{R})$. We guarantee the tight frame property of the system by requiring its adjoint system to have the orthogonality property. Implicitly, the duality principle plays role here. The interested reader should find the details from [37, 35].

It appears in Theorem 1 that in order to apply UEP for constructing MRA-based wavelet tight frames, one needs to first construct the refinement mask a_0 of a refineable function in $L_2(\mathbb{R})$ that generates an MRA. Since in general an arbitrary mask a_0 cannot guarantee that it will admit a refinable function in $L_2(\mathbb{R})$, it seems that the UEP condition (13) on the masks $\{a_0, \ldots, a_r\}$ does not automatically admit a wavelet tight frame. Indeed, it is shown in [35, Section 5.4] that a finitely supported mask a_0 with $\widehat{a}_0(0) = 1$ will admit a refinable function in $L_2(\mathbb{R})$ if the mask a_0, together with other mask $\{a_\ell\}_{\ell=1}^r$, satisfies the UEP condition (13). In other words, as long as we can construct a finitely support filter bank $\{a_0, a_1, \ldots, a_r\}$ such that the filter bank satisfies (i) $\sum_{n\in\mathbb{Z}} a_0(n) = 1$ and (ii) UEP condition (13), the filter bank $\{a_\ell\}_{\ell=0}^r$ will admit an MRA-based wavelet tight frame for $L_2(\mathbb{R})$. As a result, we have in hand a filter bank based efficient numerical implementation of multi-level decomposition and reconstruction for signals in $\ell_2(\mathbb{Z})$.

3. Main results

Consider a discrete Gabor system generated by a finitely supported window sequence $g \in \ell_2(\mathbb{Z})$:

$$\{g(m-ak)e^{-2\pi ib\ell m}, m \in \mathbb{Z}\}_{k\in\mathbb{Z},\ell\in\{0,\ldots,\frac{1}{b}-1\}},$$

with shift parameters a, b. Such a system can also be generated by the translations of $M(=\frac{1}{b})$ atoms $\{g_\ell\}_{\ell=0}^{\frac{1}{b}-1} \subset \ell_2(\mathbb{Z})$ defined by

$$g_\ell(m) = g(m)e^{-2\pi ib\ell m}, \quad m \in \mathbb{Z}. \tag{15}$$

Without loss of generality, we assume that $g(m) = 0$, for all $m \notin [0, N-1] \cap \mathbb{Z}$. Given such a Gabor system, we consider a wavelet system whose dilation factor $p = a$. That is, we define a p-refinable function (or distribution) ϕ:

$$\phi(x) = p\sum_{m\in\mathbb{Z}} g(m)\phi(px-m), \quad x \in \mathbb{R}, \tag{16}$$

and a set of wavelets $\Psi = \{\psi_\ell\}_{\ell=1}^{\frac{1}{b}-1}$ by

$$\psi_\ell(x) = p\sum_{m\in\mathbb{Z}} g_\ell(m)\phi(px-m), \quad x \in \mathbb{R}, \tag{17}$$

for $\ell = 1, \ldots, \frac{1}{b}-1$. Let $X(\Psi)$ denote a p-dilation wavelet system defined by

$$X(\Psi) = \{\psi_{\ell,n,k}\}_{\substack{1\le\ell\le\frac{1}{b}-1\\ n,k\in\mathbb{Z}}} = \{p^{n/2}\psi_\ell(p^n\cdot-k)\}_{\substack{1\le\ell\le\frac{1}{b}-1\\ n,k\in\mathbb{Z}}}. \tag{18}$$

In the next, we present a UEP-based sufficient condition on the window sequence g such that the wavelet system $X(\Psi)$ defined above forms an MRA-based tight wavelet frame for $L_2(\mathbb{R})$.

3.1. Discrete Gabor filters and MRA-based wavelet tight frames

Theorem 2. *Consider a finitely supported sequence $g \in \ell_2(\mathbb{Z})$. The function ϕ defined by* (16) *generates an MRA for $L_2(\mathbb{R})$ and the wavelet system $X(\Psi)$ defined by* (17) *and* (18) *forms a tight frame for $L_2(\mathbb{R})$, if the following conditions hold true:*

(i) $\frac{1}{b} \ge N$;

(ii) $\sum_{n\in\mathbb{Z}} g(n) = 1$;

(iii) $\sum_{n\in\Omega_j} |g(n)|^2 = \frac{b}{p}$, *for any* $\Omega_j = (p\mathbb{Z}+j) \cap [0, N-1]$ *and* $j \in \mathbb{Z}/p\mathbb{Z}$.

Proof. Before proceeding to prove that the function ϕ generates an MRA for $L_2(\mathbb{R})$ and $X(\Psi)$ forms an MRA-based tight frame for $L_2(\mathbb{R})$, we first show that the UEP condition (14) of masks $\{g_\ell\}_{\ell=0}^{1/b-1}$ holds true, provided that Condition (i), (ii) and (iii) are satisfied.

Since $g(m) = 0$ for $m < 0$ or $m \geq N$, we have $g_\ell(m) = 0$ for $\ell = 0, \ldots, \frac{1}{b} - 1$. Then, we immediately have

$$\sum_{\ell=0}^{\frac{1}{b}-1} \sum_{n\in\Omega_j} \overline{g_\ell(n)} g_\ell(n+m) = 0,$$

for any $m \notin [1-N, N-1]$. Moreover, if $1 \leq m \leq N-1$, Condition (i), $\frac{1}{b} \geq N$, gives

$$\sum_{\ell=0}^{\frac{1}{b}-1} e^{-2\pi imb\ell} = 0.$$

Thus, for $1 \leq m \leq N-1$,

$$\sum_{\ell=0}^{\frac{1}{b}-1} \sum_{n\in\Omega_j} \overline{g_\ell(n)} g_\ell(n+m) = \sum_{n\in\Omega_j} \sum_{\ell=0}^{\frac{1}{b}-1} \overline{g_\ell(n)} g_\ell(n+m) = \sum_{n\in\Omega_j} \overline{g(n)} g(n+m) \sum_{\ell=0}^{\frac{1}{b}-1} e^{-2\pi imb\ell} = 0.$$

The same equalities hold for $1-N \leq m \leq -1$. For $m = 0$, by Condition (iii), we have

$$\sum_{\ell=0}^{\frac{1}{b}-1} \sum_{n\in\Omega_j} \overline{g_\ell(n)} g_\ell(n+m) = \sum_{n\in\Omega_j} \overline{g(n)} g(n+m) \sum_{\ell=0}^{\frac{1}{b}-1} e^{-2\pi imb\ell} = \frac{1}{b} \sum_{n\in\Omega_j} |g(n)|^2 = \frac{1}{p}.$$

Therefore, Condition (14) holds for any integer $m \in \mathbb{Z}$.

Now, we show that as long as a finitely supported mask g satisfies Condition (ii) and UEP condition (14) (or equivalently (13)), it will admit a compactly supported refinable function ϕ in $L_2(\mathbb{R})$ with $\widehat{\phi}(0) = 1$, and it generates an MRA for $L_2(\mathbb{R})$. The proof is parallel to that stated in [35, Section 5.4] for the case $p = 2$. Consider the matrix

$$G = \begin{pmatrix} \widehat{g_0}(\xi) & \cdots & \widehat{g_{\frac{1}{b}-1}}(\xi) \\ \widehat{g_0}(\xi + \frac{2\pi}{p}) & \cdots & \widehat{g_{\frac{1}{b}-1}}(\xi + \frac{2\pi}{p}) \\ \vdots & \ddots & \vdots \\ \widehat{g_0}(\xi + \frac{2\pi(p-1)}{p}) & \cdots & \widehat{g_{\frac{1}{b}-1}}(\xi + \frac{2\pi(p-1)}{p}) \end{pmatrix}.$$

By the row orthonormality stated by UEP condition (13), the matrix G can be completed to a unitary matrix by adding more rows for almost all ξ. Therefore, the norm of each column in G is at most one, i.e.

$$\sum_{\mu=0}^{p-1} |\widehat{g_\ell}(\xi + \frac{2\pi\mu}{p})|^2 \leq 1 \tag{19}$$

for a.e. $\xi \in \mathbb{R}$ and $\ell = 0, ..., \frac{1}{b} - 1$. Define

$$\widehat{f_n}(\xi) = \widehat{g_0}(p^{-1}\xi)\widehat{f_{n-1}}(p^{-1}\xi) = \prod_{j=1}^{n} \widehat{g_0}(p^{-j}\xi)\widehat{f_0}(p^{-n}\xi),$$

where $\widehat{f_0} = \mathbb{1}_{[-\pi,\pi]}$. Recall that g_0 is finitely supported and satisfies Condition (ii). The pointwise limit $\widehat{\phi}$ of $\{\widehat{f_n}\}_n$ satisfies the refinement equation $\widehat{\phi}(p\xi) = \widehat{g_0}(\xi)\widehat{\phi}(\xi)$ with $\widehat{\phi}(0) = 1$. And ϕ is a compactly

supported distribution. Furthermore,

$$\begin{aligned}\|\widehat{f_n}\|^2 &= \int_{-\pi p^n}^{\pi p^n} |\prod_{j=1}^{n} \widehat{g_0}(p^{-j}\xi)|^2 d\xi \\ &= \int_{0}^{2\pi p^n} |\prod_{j=1}^{n} \widehat{g_0}(p^{-j}\xi)|^2 d\xi \\ &= \sum_{\mu=0}^{p-1} \int_{2\mu\pi p^{n-1}}^{2(\mu+1)\pi p^{n-1}} |\prod_{j=1}^{n} \widehat{g_0}(p^{-j}\xi)|^2 d\xi \\ &= \int_{0}^{2\pi p^{n-1}} |\prod_{j=1}^{n-1} \widehat{g_0}(p^{-j}\xi)|^2 \left(\sum_{\mu=0}^{p-1} |\widehat{g_0}(p^{-n}\xi + \frac{2\pi\mu}{p})| \right) d\xi.\end{aligned}$$

Then, by (19) with $\ell = 0$, we have

$$\|\widehat{f_n}\|^2 \leq \int_{0}^{2\pi p^{n-1}} |\prod_{j=1}^{n-1} \widehat{g_0}(p^{-j}\xi)|^2 d\xi = \|\widehat{f_{n-1}}\|^2.$$

By induction,

$$\|\widehat{f_n}\|^2 \leq \|\widehat{f_0}\|^2 = 2\pi,$$

for all $n \geq 0$. Since $\{\widehat{f_n}\}_n$ converges to $\widehat{\phi}$ pointwise, by Fatou's lemma,

$$\|\widehat{\phi}\|^2 \leq \liminf_{n\to\infty} \|\widehat{f_n}\|^2 \leq 2\pi,$$

and $\phi \in L_2(\mathbb{R})$. Therefore, such a refinable function ϕ generates an MRA for $L_2(\mathbb{R})$. At last, by Theorem 1, we have that the system $X(\Psi)$ defined by (17) and (18) forms a tight frame for $L_2(\mathbb{R})$. □

Theorem 2 says that once we can construct the finitely supported window sequence $g \in \ell_2(\mathbb{Z})$ satisfying Condition (ii) and Condition (iii), we immediately have an MRA-based wavelet tight frame $X(\Psi)$ using the set of wavelets Ψ of the form (17). In the next, we give a sufficient and necessary condition on finitely supported sequences g that satisfy Condition (i), (ii) and (iii).

Proposition 1. *A finitely supported sequence $g \in \ell_2(\mathbb{Z})$ satisfies Condition (i), (ii) and (iii) in Theorem 2 for some constant integer b, if and only if $g = M^{-1}(\ldots, 0, 0, \underbrace{1, ..., 1}_{M}, 0, 0, \ldots)$, where $M/p \in \mathbb{Z}^+$. In particular, if $g = M^{-1}(\ldots, 0, 0, \underbrace{1, ..., 1}_{M}, 0, 0, \ldots)$ and $M = p$, the wavelet system $X(\Psi)$ defined by* (17) *and* (18) *forms an orthonormal basis for $L_2(\mathbb{R})$.*

Proof. If $g = M^{-1}(\ldots, 0, 0, \underbrace{1, ..., 1}_{M}, 0, 0, \ldots)$ and dilation factor p is a factor of M, it can be seen that Condition (i), (ii) and (iii) hold true and $\frac{1}{b} = M$. Conversely, if Condition (i), (ii) and (iii) in Theorem 2 hold true, we have

$$\sum_{m=0}^{N-1} |g(m)|^2 = \sum_{j\in\mathbb{Z}/p\mathbb{Z}} \sum_{m\in\Omega_j} |g(m)|^2 = b$$

and

$$\sum_{m=0}^{N-1} |g(m) - \frac{1}{N}|^2 = \sum_{m=0}^{N-1} \left(|g(m)|^2 - \frac{1}{N}(g(m) + g^*(m)) \right) + \frac{1}{N^2} \cdot N = b - \frac{1}{N} \leq 0.$$

The last inequality comes from Condition (i). Thus, we have $N = \frac{1}{b} = M$, and $g(m) = \frac{1}{M}$ for any $m \in [0, N-1] \cap \mathbb{Z}$. Moreover, when M/p is not a positive integer, the sequences g with the form above cannot satisfy Condition (iii). Therefore, M must have a factor p.

In the case $M = p$, the refinable function is given by $\phi(x) = \mathbb{1}_{[0,1]}(x)$. Then for any $0 \le \ell \le M-1$,

$$\|\psi_\ell\|_2^2 = p^2 \int_{\mathbb{R}} |\sum_{m=0}^{M-1} g_\ell(m)\phi(px-m)|^2 dx = p^2 \sum_{m=0}^{M-1} \int_{\frac{m}{p}}^{\frac{m+1}{p}} |g_\ell(m)\phi(px-m)|^2 dx = M \int_0^{\frac{1}{p}} |\phi(px)|^2 dx = 1.$$

Therefore, by the result from [30], the tight frame $X(\Psi)$ is an orthonormal basis for $L_2(\mathbb{R})$. □

If $g = M^{-1}(\ldots, 0, 0, \underbrace{1, ..., 1}_{M}, 0, 0, \ldots)$, $q = M/p$ is defined as the redundancy of system $X(\Psi)$. In the special case $M = p$ and $q = 1$, the orthonormal basis $X(\Psi)$ has redundancy 1, and the refinable function admitted by such a mask is the indicator function of the MRA associated with Haar wavelet basis of dilation p. When $M > p$, the associated refinable function is not the indicator function any more. The next proposition shows the smoothness of such refinable functions.

Proposition 2. *Consider a refinable function ϕ defined by the mask $g = p^{-k}(1, ..., 1) \in \mathbb{R}^{p^k}$ for some integer $k \ge 2$ and $\widehat{\phi}(0) = 1$. Then, the function ϕ is a $(k-1)$-th order spline $\in C^{k-2}(\mathbb{R})$.*

Proof. The proof is done by induction. Let $g^k = p^{-k}(1, ..., 1)$. By Theorem 2, it admits a compactly supported refinable function $\phi_k \in L_2(\mathbb{R})$ with $\widehat{\phi_k}(0) = 1$. We first derive a recurrence equation between ϕ_k and ϕ_{k-1}. By the definition of ϕ_k and the fact that $\widehat{\phi_k}(0) = 1$, we have

$$\widehat{\phi_k}(\xi) = \prod_{j=1}^{+\infty} \widehat{g^k}(p^{-j}\xi).$$

As the length of g^k is kth power of dilation factor p, $\widehat{g^k}$ can be factorized as

$$\widehat{g^k}(\xi) = \prod_{s=0}^{k-1} \frac{1}{p} (\sum_{n=0}^{p-1} e^{-ip^s n\xi}).$$

Define $\widehat{a^s}(\xi) = \frac{1}{p}\sum_{n=0}^{p-1} e^{-ip^s n\xi}$, i.e. $a^s(p^s n) = \frac{1}{p}$ for $n = 0, .., p-1$, and $a^s(m) = 0$ otherwise. Then, it can be seen that

$$\widehat{\phi_k}(\xi) = \prod_{j=1}^{+\infty}\prod_{s=0}^{k-1} \widehat{a^s}(p^{-j}\xi) = \prod_{s=0}^{k-1}\prod_{j=1}^{+\infty} \widehat{a^s}(p^{-j}\xi) = \prod_{s=0}^{k-1} \widehat{h_s}(\xi),$$

where $h_s = p^{-s}\mathbb{1}_{[0,p^s]}$ is the refinable function corresponding to mask a^s. It implies

$$\phi_k(x) = p^{-\frac{k(k-1)}{2}} \mathbb{1}_{[0,1]} \star \mathbb{1}_{[0,p]} \star \cdots \star \mathbb{1}_{[0,p^{k-1}]}(x) = p^{1-k}\phi_{k-1} \star \mathbb{1}_{[0,p^{k-1}]}(x), \tag{20}$$

where $\star$ denotes the usual convolution operator in $\ell_2(\mathbb{Z})$.

When $k = 2$, a direct calculation gives

$$\phi_2(x) = \frac{1}{p}\mathbb{1}_{[0,1]} \star \mathbb{1}_{[0,p]} = \begin{cases} \frac{1}{p}x, & x \in [0,1), \\ \frac{1}{p}, & x \in [1,p), \\ \frac{1}{p}(p+1-x), & x \in [p,p+1), \\ 0, & \text{otherwise.} \end{cases}$$

Thus, ϕ_2 is a linear spline function and supported on $[0, p+1]$, i.e. $[0, \frac{p^2-1}{p-1}]$. By induction, suppose ϕ_{k-1} is a $(k-2)$-th order spline supported on $[0, \frac{p^{k-1}-1}{p-1}]$. Then by the recursive relationship (20), we have

$$\phi_k'(x) = p^{1-k} \int_{\mathbb{R}} \phi_{k-1}'(x-t)\mathbb{1}_{[0,p^{k-1}]}(t)dt = p^{1-k} \int_0^{p^{k-1}} \phi_{k-1}'(x-t)dt = p^{1-k}\left(\phi_{k-1}(x) - \phi_{k-1}(x-p^{k-1})\right).$$

In other words, ϕ_k' is a $(k-2)$-th order spline supported on $[0, \frac{p^{k-1}-1}{p-1} + p^{k-1}]$, which implies that ϕ_k is a $(k-1)$-th order spline supported on $[0, \frac{p^k-1}{p-1}]$. The proof is complete. □

Once we have an MRA-based wavelet tight frame constructed via the UEP, a filter bank based implementation is available for K-level decomposition and reconstruction of discrete signals. Let $\star$ denote the usual convolution operator in $\ell_2(\mathbb{Z})$. Let $\downarrow_p$ denote the down-sampling operator defined by $(f\downarrow_p)(m) = f(pm), m \in \mathbb{Z}$, and $\uparrow_p$ the up-sampling operator, the adjoint operator of down-sampling operator. Then, given a signal $f \in \ell_2(\mathbb{Z})$, the K-level wavelet decomposition can be recursively computed as follows: $c_{0,0} = f$, for $k = 1, \dots K-1$,

$$\begin{cases} c_{0,k} = \left(\sqrt{p} \cdot \overline{g_0(-\cdot)} \star c_{0,k-1}\right)\downarrow_p, \\ c_{\ell,k} = \left(\sqrt{p} \cdot \overline{g_\ell(-\cdot)} \star c_{0,k-1}\right)\downarrow_p, \quad \ell = 1, ..., r. \end{cases} \tag{21}$$

The reconstruction of f from the high-pass wavelet coefficients $(\{c_{\ell,k}\}_{0\le k\le K-1, 1\le \ell\le r})$ and the low-pass coefficient $(\{c_{0,K}\})$ is done in the same recessive way: for $k = K, K-1, ..., 1$,

$$c_{0,k-1} = \sqrt{p}\sum_{\ell=0}^{r} g_\ell \star (c_{\ell,j} \uparrow_p). \tag{22}$$

It can be seen that such a K-level wavelet decomposition expands the signal over a discrete tight frame for $\ell_2(\mathbb{Z})$ defined by

$$\left\{\{\phi_K(\cdot - p^K j)\}_{j\in\mathbb{Z}}, \{\psi_{1,k}(\cdot - p^k j)\}_{1\le k\le K, j\in\mathbb{Z}}, \dots, \{\psi_{r,k}(\cdot - p^k j)\}_{1\le k\le K, j\in\mathbb{Z}}\right\}, \tag{23}$$

where $\phi_K, \psi_{\ell,k}$ are sequences defined by

$$\widehat{\phi_K}(\omega) = \sqrt{p}\prod_{j=0}^{K-1}\widehat{g}_0(p^j\omega), \text{and} \quad \widehat{\psi_{\ell,k}} = \sqrt{p}\widehat{g}_\ell(p^{k-1}\omega)\prod_{j=0}^{k-1}\widehat{g}_0(p^j\omega),$$

for $\ell = 1, \dots, r, k = 1, \dots, K$. The tight frame defined by (23) with the masks $\{g_\ell\}_{\ell=0}^{\frac{1}{b}-1}$ of the form (15) indeed can be viewed as a discrete tight Gabor frame for $\ell_2(\mathbb{Z})$ with K-level multi-scale structure. When $K = 1$, the tight frame defined by (23) can be expressed as

$$\{\sqrt{p}g_\ell(m - pk) = \sqrt{p}g(m - pk)e^{-2\pi ib\ell m}\}_{0\le\ell\le\frac{1}{b}-1, k\in\mathbb{Z}},$$

which exactly is the Gabor tight frames for $\ell_2(\mathbb{Z})$ defined in (8) with $a = p$.

Example 1. *When taking $M = 4$ and $p = 2$, we have $g_0 = g = (\frac{1}{4}, \frac{1}{4}, \frac{1}{4}, \frac{1}{4})$, and the other three Gabor atoms, $g_1 = (\frac{1}{4}, -\frac{1}{4}i, -\frac{1}{4}, \frac{1}{4}i), g_2 = (\frac{1}{4}, -\frac{1}{4}, \frac{1}{4}, -\frac{1}{4})$ and $g_3 = (\frac{1}{4}, \frac{1}{4}i, -\frac{1}{4}, -\frac{1}{4}i)$. The refinable function ϕ with the mask g is a linear spline given by*

$$\phi(x) = \begin{cases} \frac{1}{2}x, & x \in [0, 1), \\ \frac{1}{2}, & x \in [1, 2), \\ \frac{1}{2}(3 - x), & x \in [2, 3), \\ 0, & \textit{otherwise.} \end{cases}$$

See Figure 1 for the plots of the refinable ϕ and three framelets admitted by g_1, g_2, g_3.

Example 2. *When taking $M = 6$ and $p = 2$, we have $g = (\frac{1}{6}, \frac{1}{6}, \frac{1}{6}, \frac{1}{6}, \frac{1}{6}, \frac{1}{6})$. The associated refinable function is continuous but is not a spline. See Figure 2 for the plots of the refinable ϕ and five framelets.*

Example 3. *When Taking $M = 8$ and $p = 2$, we have $g = (\frac{1}{8}, \frac{1}{8}, \frac{1}{8}, \frac{1}{8}, \frac{1}{8}, \frac{1}{8}, \frac{1}{8}, \frac{1}{8})$. The corresponding*

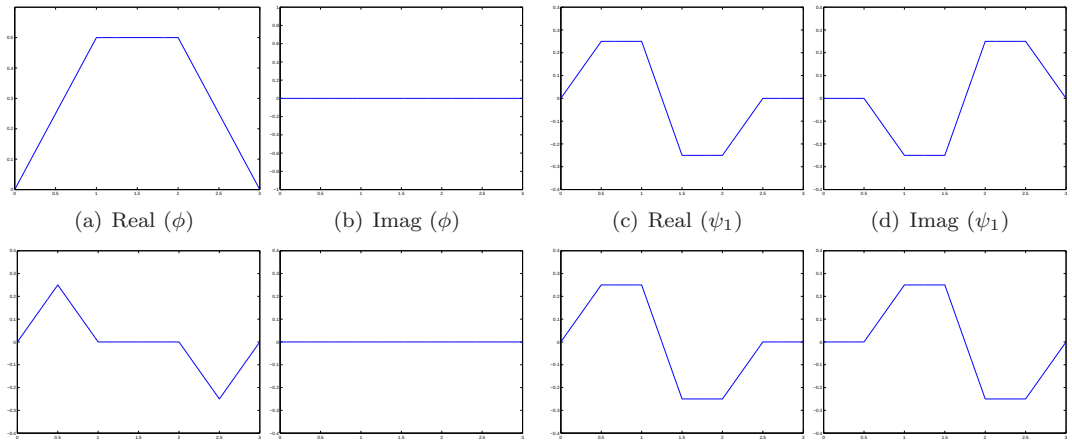

(a) Real (ϕ) (b) Imag (ϕ) (c) Real (ψ_1) (d) Imag (ψ_1)

(e) Real (ψ_2) (f) Image (ψ_2) (g) Real (ψ_3) (h) Image (ψ_3)

Figure 1: The real part and imaginary part of the refinable function and three framelets generated from $g = (\frac{1}{4}, \frac{1}{4}, \frac{1}{4}, \frac{1}{4})$, if $p = 2$.

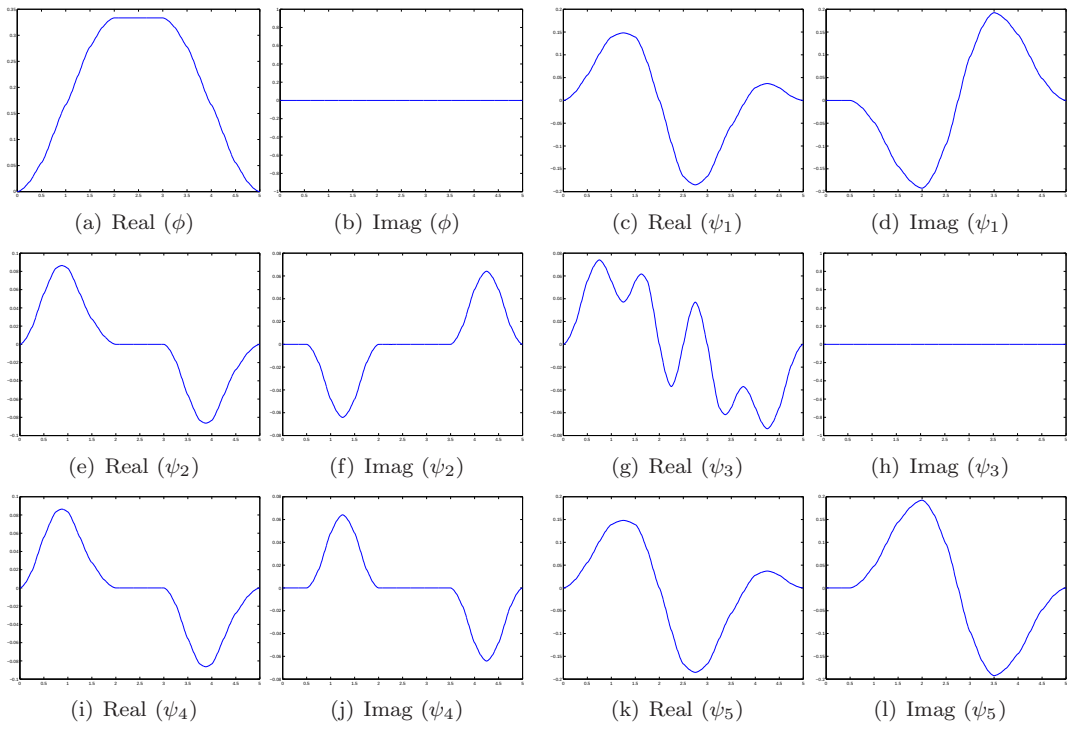

(a) Real (ϕ) (b) Imag (ϕ) (c) Real (ψ_1) (d) Imag (ψ_1)

(e) Real (ψ_2) (f) Imag (ψ_2) (g) Real (ψ_3) (h) Imag (ψ_3)

(i) Real (ψ_4) (j) Imag (ψ_4) (k) Real (ψ_5) (l) Imag (ψ_5)

Figure 2: The real part and imaginary part of the refinable function and five framelets generated from $g_0 = (\frac{1}{6}, \frac{1}{6}, \frac{1}{6}, \frac{1}{6}, \frac{1}{6}, \frac{1}{6})$, if $p = 2$.

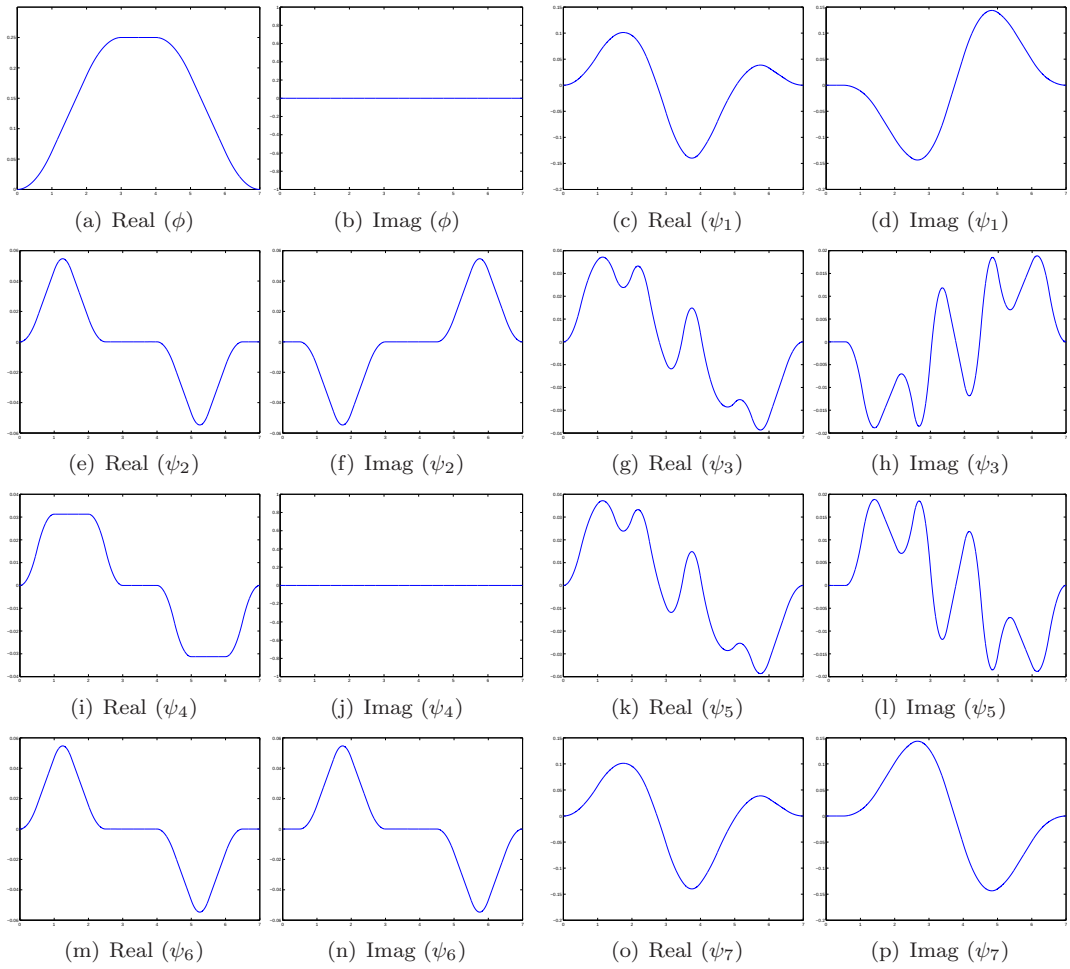

(a) Real (ϕ) (b) Imag (ϕ) (c) Real (ψ_1) (d) Imag (ψ_1)

(e) Real (ψ_2) (f) Imag (ψ_2) (g) Real (ψ_3) (h) Imag (ψ_3)

(i) Real (ψ_4) (j) Imag (ψ_4) (k) Real (ψ_5) (l) Imag (ψ_5)

(m) Real (ψ_6) (n) Imag (ψ_6) (o) Real (ψ_7) (p) Imag (ψ_7)

Figure 3: The real part and imaginary part of the refinable function and seven framelets generated from $g_0 = (\frac{1}{8}, \frac{1}{8}, \frac{1}{8}, \frac{1}{8}, \frac{1}{8}, \frac{1}{8}, \frac{1}{8}, \frac{1}{8})$, if $p = 2$.

refinable function is a quadratic spline given by

$$\phi(x) = \begin{cases} \frac{1}{16}x^2 & x \in [0,1], \\ \frac{x}{8} - \frac{1}{16} & x \in [1,2], \\ \frac{1}{16}(-x^2 + 6x - 5) & x \in [2,3], \\ \frac{1}{4} & x \in [3,4], \\ \frac{1}{16}(-x^2 + 8x - 12) & x \in [4,5], \\ -\frac{x}{8} + \frac{13}{16} & x \in [5,6], \\ \frac{1}{16}(x-7)^2 & x \in [6,7], \\ 0 & \textit{otherwise.} \end{cases}$$

See Figure 3 for the plots of the refinable ϕ and seven framelets.

Before ending this section, we would like to mention that the construction scheme presented in this section can also be used for constructing real-valued discrete tight frame formed by local Cosine basis with MRA structure. Consider atoms defined from a local Cosine basis with even support M:

$$g_\ell(m) = \frac{1}{\lambda_\ell} \cos(\frac{\pi(2m+1)\ell}{2M}), \quad 0 \le m \le M-1,$$

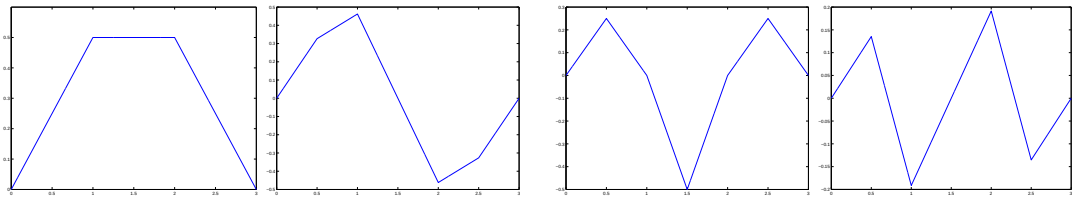

(a) ϕ (b) ψ_1 (c) ψ_2 (d) ψ_3

Figure 4: wavelets generated from $g_0 = (\frac{1}{4}, \frac{1}{4}, \frac{1}{4}, \frac{1}{4})$ and cosine basis, if $p = 2$.

where $\lambda_0 = M$, and $\lambda_\ell = \frac{M}{\sqrt{2}}$ for $1 \le \ell \le M-1$. By a direct calculation, these atoms satisfy the UEP if being used as the refinement mask and wavelet masks. Thus, the system generated by these masks using (23) forms a tight frame for $\ell_2(\mathbb{Z})$. The refinable function admitted by g_0 generated the same MRA as that of tight Gabor frames, but the resulting wavelet tight frames are different as the framelets are different. For example, when taking $M = 4$ and $p = 2$, we have

$$\begin{cases} g_0 = (\frac{1}{4}, \frac{1}{4}, \frac{1}{4}, \frac{1}{4}), \\ g_1 = \frac{\sqrt{2}}{4}(\cos\frac{\pi}{8}, \cos\frac{3\pi}{8}, \cos\frac{5\pi}{8}, \cos\frac{7\pi}{8}), \\ g_2 = \frac{\sqrt{2}}{4}(\cos\frac{\pi}{4}, \cos\frac{3\pi}{4}, \cos\frac{5\pi}{4}, \cos\frac{7\pi}{4}), \\ g_3 = \frac{\sqrt{2}}{4}(\cos\frac{3\pi}{8}, \cos\frac{7\pi}{8}, \cos\frac{\pi}{8}, \cos\frac{5\pi}{8}). \end{cases}$$

See Figure 4 for the plots of the refinable ϕ and three framelets.

3.2. (Tight) Gabor frames induced from refinable functions

In the previous section, special discrete Gabor tight frames in signal space are linked to the MRA-based wavelet tight frames in square integrable function space, which brings MRA structure to discrete Gabor frames. Another interesting question is when can we link Gabor tight frames in square integrable function space to the MRA as well. In other words, what is the link between a refinable function to the window function of a tight Gabor frame?

Using the sampling rate $a = p = 2$ and $b = \frac{1}{M}$ as discrete tight Gabor frames with MRA structure, we define a Gabor system on the lattices: $K = 2\mathbb{Z}$, $L = \frac{1}{M}\mathbb{Z}$:

$$(K, L)_g = \{g(x - 2k)e^{-\frac{2\pi i \ell x}{M}}, x \in \mathbb{R}\}_{k,\ell\in\mathbb{Z}}, \tag{24}$$

where $g \in L_2(\mathbb{R})$ is a compactly supported non-negative window function. Suppose that $\mathrm{supp}(g) \subseteq [0, \gamma]$ and $g > 0$ on $(0, \gamma)$ for some positive constant γ. It is shown, e.g. [27, pp. 24], that the system $\{g(x - ak)e^{-2\pi i b\ell x}\}_{k,\ell\in\mathbb{Z}}$ generated by such a window function forms a tight frame for $L_2(\mathbb{R})$ if and only if the following two conditions hold true:

(a) $\gamma b \le 1$;

(b) $\sum_{k\in\mathbb{Z}} |g(\cdot - ak)|^2$ is non-zero constant.

Based on the result above, we give a sufficient condition on a refinable function ϕ so that the Gabor system defined as (24) will form a frame when $g = \phi$ and it will form a tight frame when $g = \sqrt{2\phi/M}$.

Theorem 3. *Let $\phi \in L_2(\mathbb{R})$ with $\widehat{\phi}(0) = 1$ be a continuous refinable function supported on $[0, M-1]$. Suppose that $M \ge 4$ and $\phi(x) > 0$ for any $x \in (0, M-1)$. Let g_0 denotes its refinement mask. Then, the Gabor system $(K, L)_g$ with $g = \phi$ forms a frame for $L_2(\mathbb{R})$. Further, suppose the mask g_0 satisfies*

$$\sum_{m\in\Lambda_j} g_0(m) = \frac{1}{4}, \tag{25}$$

where $j \in \mathbb{Z}/4\mathbb{Z}$ and $\Lambda_j = (4\mathbb{Z} + j) \cap [0, M-1]$. Then, the Gabor system $(K, L)_g$ with $g = \sqrt{2\phi/M}$ forms a tight frame for $L_2(\mathbb{R})$.

Proof. The frame property of the Gabor system $(K, L)_\phi$ is proved by one sufficient condition presented in [27] which states that as long as the window function ϕ is continuous on its support $[0, M-1]$, $\phi > 0$ on $(0, M-1)$, and $b = \frac{1}{M} \leq \frac{1}{M-1}$, the system $(K, L)_\phi$ forms a frame for $L_2(\mathbb{R})$. For the tight frame property, since $b = \frac{1}{M} \leq \frac{1}{M-1}$, Condition (a) is satisfied. For any $j \in \mathbb{Z}$ and $r \in \mathbb{N}$,

$$\sum_{k\in\mathbb{Z}} \phi(\frac{j}{2^r} - 2k) = \sum_{k\in\mathbb{Z}} \sum_{m\in\mathbb{Z}} 2g_0(m)\phi(\frac{j}{2^{r-1}} - 4k - m) = \sum_{k\in\mathbb{Z}} \sum_{m\in\mathbb{Z}} 2g_0(m-4k)\phi(\frac{j}{2^{r-1}} - m).$$

As both g_0 and ϕ are compactly supported, one then can change the order of finite summations which gives

$$\sum_{k\in\mathbb{Z}} \phi(\frac{j}{2^r} - 2k) = \sum_{m\in\mathbb{Z}} \sum_{k\in\mathbb{Z}} 2g_0(m-4k)\phi(\frac{j}{2^{r-1}} - m) = \frac{1}{2} \sum_{m\in\mathbb{Z}} \phi(\frac{j}{2^{r-1}} - m).$$

Here, the last equality comes from (25). Moreover, by (25), we have $\sum_{k\in\mathbb{Z}} g_0(m-4k) = \sum_{k\in\mathbb{Z}} g_0(m-4k+2) = \frac{1}{4}$, and thus $\sum_{k\in\mathbb{Z}} g_0(m-2k) = \frac{1}{2}$. By the same argument above, we have

$$\sum_{m\in\mathbb{Z}} \phi(\frac{j}{2^{r-1}} - m) = \sum_{n\in\mathbb{Z}} \sum_{m\in\mathbb{Z}} 2g_0(n-2m)\phi(\frac{j}{2^{r-2}} - n) = \sum_{n\in\mathbb{Z}} \phi(\frac{j}{2^{r-2}} - n)$$

Repeat this process, one obtains

$$\sum_{m\in\mathbb{Z}} \phi(\frac{j}{2^{r-1}} - m) = \sum_{n\in\mathbb{Z}} \phi(\frac{j}{2^{r-2}} - n) = \cdots = \sum_{n\in\mathbb{Z}} \phi(j-n) = \sum_{n\in\mathbb{Z}} \phi(n).$$

Recall that we have

$$\widehat{\phi}(0) = \int_{-\infty}^{+\infty} \phi(t)dt = \sum_{n\in\mathbb{Z}} \phi(n),$$

when the function ϕ is a continuous refinable function. By the fact that $\widehat{\phi}(0) = 1$, we have then

$$\sum_{k\in\mathbb{Z}} \phi(\frac{j}{2^r} - 2k) = 1/2,$$

for any $j \in \mathbb{Z}$ and $r \in \mathbb{N}$. Since $\{\frac{j}{2^r}, j \in \mathbb{Z}, r \in \mathbb{N}\}$ is dense in $\mathbb{R}$ and the continuity of ϕ implies the continuity of $\sum_{k\in\mathbb{Z}} \phi(\cdot - 2k)$, it is established that for any $x \in \mathbb{R}$,

$$\sum_{k\in\mathbb{Z}} \phi(x - 2k) = 1/2,$$

which is exactly Condition (b) with $a = 2$. Thus, by the result in [27, pp. 24], the Gabor system $(K, L)_g$ defined as (24) with $g = \sqrt{2\phi/M}$ forms a tight frame for $L_2(\mathbb{R})$. □

Example 4. *Consider the masks in Example 1 and Example 3, i.e.* $M = 4$, $g_0 = (\frac{1}{4}, \frac{1}{4}, \frac{1}{4}, \frac{1}{4})$ *and* $M = 8$, $g_0 = (\frac{1}{8}, \frac{1}{8}, \frac{1}{8}, \frac{1}{8}, \frac{1}{8}, \frac{1}{8}, \frac{1}{8}, \frac{1}{8})$. *These masks and their refinable functions* ϕ *satisfy conditions in Theorem 3. Therefore, the Gabor system with window function* $\sqrt{2\phi/M}$ *is a tight frame for* $L_2(\mathbb{R})$. *For* $M = 4$ *and* $M = 8$, $\sqrt{\phi}$ *is shown in Figure 5.*

4. Experiments on Image Recovery

In this section, we apply discrete Gabor tight frames with MRA structure constructed in the previous section in ℓ_1-norm relating regularization for image recovery. The system used for representing 2D images is generated by the tensor product of one dimensional discrete un-decimated tight Gabor frames with MRA structure constructed from Theorem 2 and Corollary 1 in Section 3. Two types of discrete Gabor tight frames constructed in this paper are evaluated in the experiments, including (1) the two-level Gabor tight frame with size $M = 4$ and dilation $p = 2$; (2) the one-level Gabor tight frame with size $M = 8$ and dilation $p = 2$.

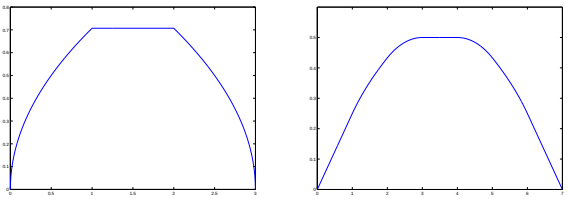

(a) $M = 4$ (b) $M = 8$

Figure 5: Two window functions for generating tight Gabor frames, using square root of the refinable functions, $\sqrt{\phi}$, constructed in Example 1 and Example 3.

(a) Barbara (b) Bowl (c) Cameraman (d) Lena

Figure 6: Four tested images

By vectorizing a 2D image as a vector in $\mathbb{R}^N$, most image recovery problems are about solving a linear inverse problem:

$$f = Hu + n, \tag{26}$$

where f denotes the observed image, u denotes the true image and n denotes noise. For image deconvolution, H is a convolution operator and H is an identity matrix for image denoising. Let W denote the decomposition operator of a K-level discrete wavelet tight frame, and its adjoint W^* the reconstruction operator. One most often seen ℓ_1-norm relating regularization for image recovery is

$$\min_{v\in\mathbb{R}^N} \|Wv\|_1, \quad \text{s.t.} \quad \|Hv - f\|_2 \le \epsilon, \tag{27}$$

where $\epsilon = \|n\|_2$. The optimization problem above can be solved via the split Bregman iteration, i.e.

$$\begin{cases} (\mu H^\top H + \lambda I)v^{k+1} = \mu H^\top (f - c^k) + \lambda W^*(d^k - b^k) \\ d^{k+1} = \mathcal{T}_{\frac{1}{\lambda}}(Wv^{k+1} + b^k), \\ b^{k+1} = b^k + Wv^{k+1} - d^{k+1}, \\ c^{k+1} = c^k + Hv^{k+1} - f, \end{cases} \tag{28}$$

where $\mathcal{T}_\delta(w) = [t_\delta(w_1), t_\delta(w_2), \ldots]^\top$ is the soft thresholding operator, with $t_\delta(w_i) = \frac{w_i}{|w_i|}\max\{0, |w_i| - \delta\}$ if $w_i \neq 0$ and $t_\delta(0) = 0$. Interesting readers are referred to [6] for more details.

The results obtained using the Gabor tight frames with MRA structures are compared to that from several other discrete systems often seen in regularizations for image recovery, including the difference operator used in the TV method (see e.g. [44]), linear spline wavelet tight frames [27] used in ℓ_1-norm relating regularization [6], the tight frame composed by two systems (local DCT and linear spline tight wavelet frame), dual-tree complex wavelet transform (DT-CWT) [8], and two-layer discrete Gabor frames constructed in [3] which are generated from the 4th order B-spline functions using $M = 7, a = 2, b = \frac{1}{7}$ and $M = 15, a = 4, b = \frac{1}{15}$. The performance of image recovery is measured in terms of the PSNR value given by

$$\text{PSNR} = -20\log_{10}\frac{\|u - \widetilde{u}\|}{255N},$$

where N denotes the total number of image pixels, u and $\widetilde{u}$ denote the truth and the result.

Table 1: PSNR values of denoised results for noisy images with noise level $\sigma = 20$

image	TV	linear spline framelet	DT-CWT	discrete Gabor frame [3]	2-level tight frames w/ $M = 4$	1-level tight frame w/ $M = 8$
Barbara512	26.84	29.25	28.90	30.39	28.07	29.38
Bowl256	29.24	30.15	29.43	30.58	30.06	30.40
Cameraman256	28.83	29.00	28.94	29.26	29.41	29.29
Lena512	30.71	31.10	31.49	31.74	31.03	31.39

Table 2: PSNR values of deblurred results for blurred images with noise level $\sigma = 3$

image	kernel	TV	linear spline framelet	DT-CWT	discrete Gabor frame [3]	2-level frames w/ $p = 4$	1-level frame w/ $p = 8$
Barbara512	disk	24.77	25.17	25.15	25.65	25.12	25.48
	motion	24.64	24.97	25.00	25.70	25.00	25.49
	gaussian	24.13	24.14	24.19	24.21	24.18	24.18
	average	23.99	24.03	24.07	24.27	24.05	24.10
Bowl256	disk	28.73	28.92	28.99	29.35	29.10	29.13
	motion	28.88	29.08	29.15	29.67	29.46	29.36
	gaussian	27.96	27.82	28.32	28.66	28.04	28.46
	average	28.73	28.84	28.94	29.25	29.12	29.21
Cameraman256	disk	26.31	26.83	26.22	27.01	27.08	26.73
	motion	26.18	27.14	26.35	26.93	27.07	26.72
	gaussian	24.96	24.84	24.73	25.04	25.06	24.94
	average	25.08	25.12	25.00	25.55	25.41	25.30
Lena512	disk	32.05	32.17	32.25	32.53	32.03	32.06
	motion	30.86	30.49	31.21	31.43	30.80	30.45
	gaussian	31.34	31.26	31.59	31.74	31.52	31.55
	average	30.10	29.96	30.21	30.36	29.91	30.06

In the experiments of image denoising, the tested images are synthesized by adding Gaussian white noise with standard deviation $\sigma = 20$ on tested images: (1) for two-level discrete Gabor tight frame with $M = 4$, set $\lambda = \frac{4}{255}$ and $\mu = \frac{1}{765}$; (2) for one-level discrete Gabor tight frame with $M = 8$, set $\lambda = \frac{8}{255}$ and $\mu = \frac{2}{765}$. See Table 1 for the summary of the PSNR values of the results denoised by different methods. And see Figure 8 for a visualization of the denoised images. In the experiments of image deconvolution, the tested images, shown in Figure 6, are firstly convoluted with a blur kernel and then added with Gaussian white noise. The standard deviation of noise is $\sigma = 3$ and four types of blur kernel are tested: (1) disk kernel of radius 3 pixels, (2) linear motion blur kernel of length 15 pixels and of orientation 30°, (3) Gaussian kernel of size 15×15 pixels and standard derivation 2, and (4) averaging kernel of size 9×9 pixels. The parameters are uniformly set for all images: (1) for two-level discrete tight Gabor frame with $M = 4$, set $\lambda = 0.05$ and $\mu = \frac{1}{4}$; (2) for one-level discrete tight Gabor frame with $M = 8$, set $\lambda = 0.2$ and $\mu = 1$. See Table 2 for the summary of PSNR values of results deblurred by different methods. See Figure 7 for a visual illustration of deconvolution results. Overall it can be seen that, in terms of the performance in image recovery, the discrete tight Gabor frames with MRA structure are comparable to non-stationary Gabor frames constructed in [3], and are slightly better than the other wavelet tight frames or TV-based regularization.

Acknowledgment

The authors would like to thank the associated editor and the reviewer for their helpful comments and suggestions. This work was partially supported by Singapore MOE AcRF Research Grant MOE2012-T3-1-108 and R-146-000-229-114.

References

[1] H. Malvar, Signal processing with lapped transform, Artech House, 1991.

[2] G. K. Wallace, The JPEG still picture compression standard, IEEE Trans. Consum. Electr. 38 (1) (1992) xviii–xxxiv.

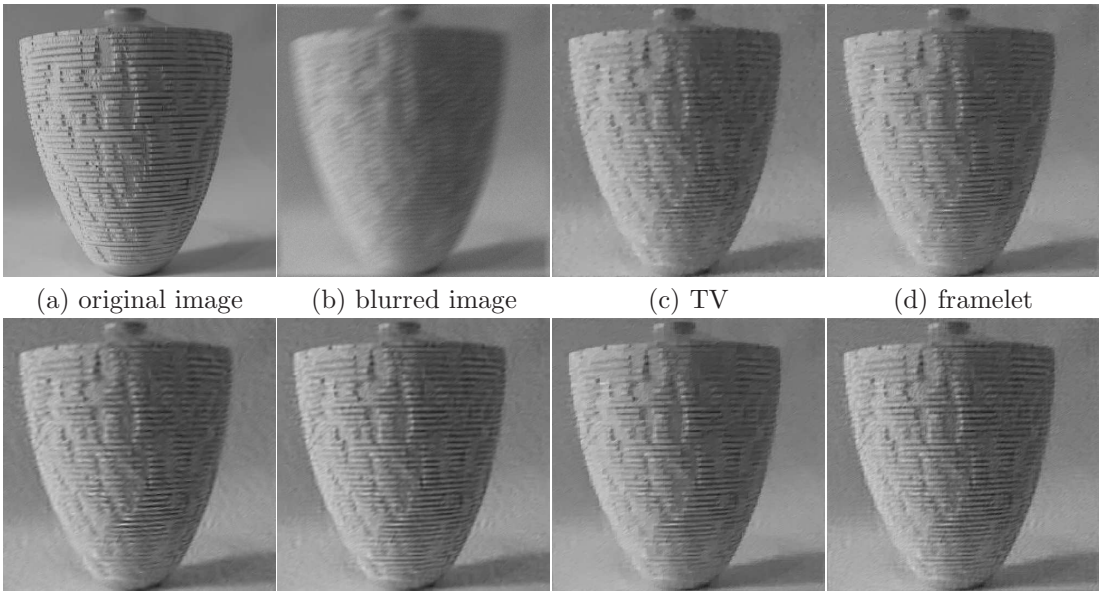

(a) original image (b) blurred image (c) TV (d) framelet

(e) DT-CWT (f) Gabor frame [3] (g) two-level, $M = 4$ (h) one-level, $M = 8$

Figure 7: Visual illustration of image deconvolution. (a) True image; (b) image blurred by motion kernel and added by noise with noise level $\sigma = 3$; (c)-(h) deblurred results by different methods.

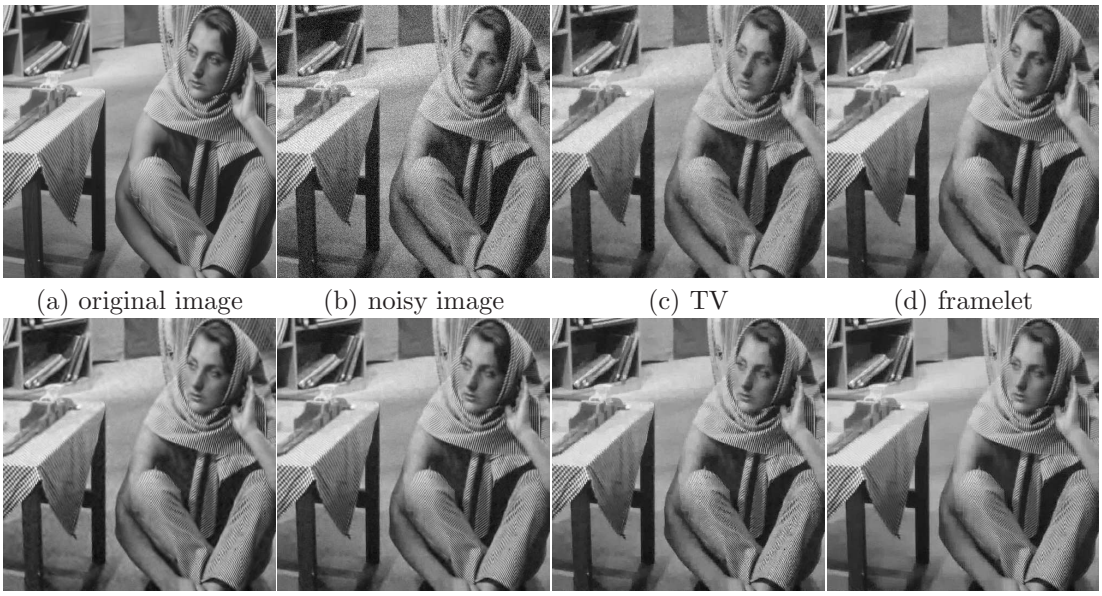

(a) original image (b) noisy image (c) TV (d) framelet

(e) DT-CWT (f) Gabor frame [3] (g) two-level, $M = 4$ (h) one-level, $M = 8$

Figure 8: Visual illustration of image denoising. (a) True image; (b) noisy image with noise level $\sigma = 20$; (c)-(h) denoised results by four different methods.

[3] H. Ji, Z. Shen, Y. Zhao, Directional frames for image recovery: multi-scale discrete Gabor frames, J. Fourier Anal. Appl.doi:10.1007/s00041-016-9487-5.

[4] R. Coifman, D. Donoho, Translation-invariant de-noising, in: Wavelet and Statistics, Vol. 103 of Springer Lecture Notes in Statistics, Springer-Verlag., 1994, pp. 125–150.

[5] J. Cai, R. Chan, Z. Shen, A framelet-based image inpainting algorithm, Appl. Comput. Harmon. Anal. 24 (2) (2008) 131–149.

[6] J. Cai, S. Osher, Z. Shen, Split Bregman methods and frame based image restoration, SIAM J: Multiscale Model. Sim. 8 (2) (2009) 337–369.

[7] J. Cai, H. Ji, C. Liu, Z. Shen, Framelet based blind image deblurring from a single image, IEEE Trans. Image Process. 21 (2) (2012) 562–572.

[8] I. W. Selesnick, R. G. Baraniuk, N. C. Kingsbury, The dual-tree complex wavelet transform, IEEE Signal Proc. Mag. 22 (6) (2005) 123–151.

[9] I. Daubechies, B. Han, A. Ron, Z. Shen, Framelets: MRA-based constructions of wavelet frames, Appl. Comput. Harmon. Anal. 14 (2003) 1–46.

[10] B. Dong, H. Ji, J. Li, Z. Shen, Y. Xu, Wavelet frame based blind image inpainting, Appl. Comput. Harmon. Anal. 32 (2) (2011) 268–279.

[11] J.-F. Cai, H. Ji, C. Liu, Z. Shen, Blind motion deblurring from a single image using sparse approximation, in: CVPR, 2009, pp. 104–111.

[12] B. Dong, J. Li, Z. Shen, X-ray ct image reconstruction via wavelet frame based regularization and radon domain inpainting, J. Sci. Comput. 54 (2-3) (2013) 333–349.

[13] M. Li, Z. Fan, H. Ji, Z. Shen, Wavelet frame based algorithm for 3d reconstruction in electron microscopy, SIAM J. Sci. Comput. 36 (1) (2014) B45–B69.

[14] J. Cai, S. Huang, H. Ji, Z. Shen, G. Ye, Data-driven tight frame construction and image denoising, Appl. Comput. Harmon. Anal. 37 (1) (2014) 89–105.

[15] Y. Quan, H. Ji, Z. Shen, Data-driven multi-scale non-local wavelet frame construction and image recovery, J. Sci. Comput. 63 (2) (2015) 307–329.

[16] J. Cai, B. Don, Z. Shen, S. Osher, Image restoration: total variation ; wavelet frames; and beyond, J. Amer. Math. Soc. 25 (4) (2012) 1033–1089.

[17] Z. Shen, Wavelet frames and image restorations, in: Proc. ICM, Vol. 4, Hindustan Book Agency, India, 2010, pp. 2834–2863.

[18] B. Dong, Z. Shen, Mra-based wavelet frames and applications, in: IAS/Park City Mathematics Series: The Mathematics of Image Processing, Vol. 19, Park City Mathematics Institute, 2010, pp. 7–185.

[19] B. Dong, Z. Shen, Image restoration: a data-driven perspective, in: L. Guo, Z. Ma (Eds.), Proc. ICIAM, High Education Press, Beijing, 2015, pp. 65–108.

[20] T. S. Lee, Image representation using 2D Gabor wavelets, IEEE Trans. Pattern Anal. 18 (10) (1996) 959–971.

[21] Y. R. Li, L. Shen, B. W. Suter, Adaptive inpainting algorithm based on DCT induced wavelet regularization, IEEE Trans. Image Process. 22 (2) (2013) 752–763.

[22] J. G. Daugmann, Two-dimensional spectral analysis of cortical receptive field profile, Vision Res. 20 (1980) 847–856.

[23] A. Grossmann, J. Morlet, Decomposition of hardy functions into square integrable wavelets of constant shape, SIAM J. Math. Anal. 15 (4) (1984) 723–736.

[24] I. Daubechies, The wavelet transform, time-frequency localization and signal analysis, IEEE Trans. Inform. Theory 36 (5) (1990) 961–1005.

[25] D. Gabor, Theory of communication, J. IEE 93 (26) (1946) 429–457.

[26] A. Ron, Z. Shen, Frames and stable bases for subspaces of $L_2(\mathbb{R}^d)$: the duality principle of Weyl-Heisenberg sets, in: M. Chu, R. Plemmons, D. Browns, D. Ellison (Eds.), Proceedings of the Lanczos Centenary Conference, Raleigh, NC, 1993, pp. 422–425.

[27] A. Ron, Z. Shen, Weyl-Heisenberg Frames and Riesz Bases in $L^2(R^d)$, Duke Math. J. 89 (1997) 237–282.

[28] A. Janssen, Duality and biorthogonality for Weyl-Heisenberg frames, J. Fourier Anal. Appl. 1 (4) (1994) 403–436.

[29] I. Daubechies, H. Landau, Z. Landau, Gabor time-frequency lattices and the Wexler-Raz identity, J. Fourier Anal. Appl. 4 (1) (1994) 437–478.

[30] A. Ron, Z. Shen, Affine system in $L_2(R^d)$: the analysis of the analysis operator, J. Funct. Anal. 148.

[31] I. Daubechies, A. Grossman, Y. Meyer, Painless non-orthogonal expansions, J. Math. Phys. 45 (1986) 1271–1283.

[32] Y. Meyer, Wavelets and operators, Vol. 1, Cambridge university press, 1995.

[33] I. Daubechies, Orthonormal bases of compactly supported wavelets, Comm. Pure Appl. Math. 40 (7) (1988) 909–996.

[34] A. Cohen, I. Daubechies, J.-C. Feauveau, Biorthogonal bases of compactly supported wavelets, Comm. Pure Appl. Math. 45 (5) (1992) 485–560.

[35] Z. Fan, A. Heinecke, Z. Shen, Duality for frames, J. Fourier Anal. Appl. 22 (1) (2016) 71–136.

[36] S. Mallat, Multiresolution approximations and wavelet orthonormal bases of $L^2(R)$, Trans. Amer. Math. Soc. 315 (1) (1989) 69–87.

[37] Z. Fan., H. Ji, Z. Shen, Dual Gramian analysis: duality principle and unitary extension principle, AMS Math. Comp. 85 (2016) 239–270.

[38] A. Ron, Z. Shen, Frames and stable bases for shift-invariant subspaces of $L_2(\mathbb{R}^d)$, Canadian J. Math. 47 (1995) 1051–1094.

[39] J. Wexler, S. Raz, Discrete gabor expansions, Signal Process. 21 (3) (1990) 207–220.

[40] I. Daubechies, The wavelet transform, time-frequency localization and signal analysis, IEEE Trans. Inform. Theory 36 (5) (1990) 961–1005.

[41] S. Li, On general frame decompositions, Numer. Func. Anal. Opt. 16 (9-10) (1995) 1181–1191.

[42] A. Janssen, From continuous to discrete Weyl-Heisenberg frames through sampling, J. Fourier Anal. Appl. 3 (5) (1997) 583–596.

[43] Z. Cvetković, M. Vetterli, Tight Weyl-Heisenberg frame in $\ell^2(Z)$, IEEE Trans. Signal Process. 46 (5) (1998) 1256–1260.

[44] Y. Wang, J. Yang, W. Yin, Y. Zhang, A new alternating minimization algorithm for total variation image reconstruction, SIAM J. Imaging Sci. 1 (3) (2008) 248–272.